



Effect of frequency of loading on vibration isolation efficiency of geocell reinforced beds

HASTHI VENKATESWARLU^{1,*} and A HEGDE²

¹Department of Civil Engineering, Indian Institute of Science, Bangalore 560012, India

²Department of Civil and Infrastructure Engineering, Indian Institute of Technology, Dharwad 580011, India
e-mail: hvenkateswar@iisc.ac.in; ahegde@iitdh.ac.in

MS received 29 August 2022; revised 17 April 2023; accepted 11 May 2023

Abstract. One of the most governing factors in the design of the foundation supporting the vibration sources is to reduce the amplitude of vibration. Vibration generated from industrial machinery is frequency dependant, and frequency has a significant influence on these design factors. Therefore, this manuscript describes the influence of frequency of loading on the vibration mitigation efficacy and the behaviour of geocell reinforced bed using the experimental and numerical studies. As part of the experimental study, a series of field vibration tests have been performed over the unreinforced and geocell-reinforced soil beds by varying the frequency of loading between 15 and 45 Hz. Using field tests, different vibration isolation parameters namely, velocity reduction ratio (VRR), vibration mitigation efficiency and attenuation coefficient have been studied. Numerical analysis has been conducted using FLAC^{3D} to demonstrate the variation of VRR with respect to some of the key parameters namely, footing shape, geocell area, and relative density of infill. From the experimental results, vibration mitigation efficiency of geocell reinforced beds corresponding to distinct frequencies of loading i.e., 15 Hz, 25 Hz, and 45 Hz was observed as 39%, 43%, and 49%, respectively. The attenuation coefficient of a geocell reinforced bed was found to increase with the increase in frequency. Use of geocell reinforcement, notably minimized the strain generated over the foundation bed. However, the strain corresponding to the unreinforced and geocell-reinforced beds was increased with the increase in frequency of loading. VRR was found to decrease with the increase in geocell area and relative density of the infill material.

Keywords. Geocell; frequency; shear strain; velocity reduction ratio; footing shape; relative density of infill.

1. Introduction

Foundation beds supporting the vibration sources are subjected to a wide range of dynamic loads. The specific examples of these sources are high-speed machinery like rotary machines and compressors. Prominently, the vibration load emanated from the machines is frequency-dependent and repetitive. Thus, examining the behaviour of foundation beds under a vibration load has been a challenging and interesting research problem in the recent past. The foundation bed plays a predominant role in mitigating all the adverse consequences produced by the induced vibration. During the operation of high-speed machines, the foundation bed may be subjected to extreme limits of vibration and strains. Excessive vibration not only jeopardize the functioning of sensitive devices but also damage the adjacent and historic buildings. The workers and people living nearby are exposed to dizziness and nausea in such circumstances [1]. Also, excessive strain minimizes the modulus of the foundation bed [2]. Consequently, the

foundation bed fails to offer enough resistance to support the load from the machine and footing. Thus, substantial attention is essential to quantify the behaviour of the foundation bed supporting the vibration sources. To date, numerous studies have employed theoretical and experimental methodologies to quantify the response of the footing under vibration loading conditions.

Baidya and Rathi [3] investigated that the increase in thickness of the foundation bed leads to the reduction in resonant frequency and increase in peak displacement amplitude. Importantly, changes in both the resonant frequency and peak displacement amplitude were found insignificant when the increase in thickness of the layer beyond three times the width of the footing. Kumar and Reddy [4] noticed the increase in displacement amplitude with the decrease in stiffness of the soil strata. Kirar *et al* [5] observed the decrease in resonant frequency and increase in resonant amplitude with the increase in the excitation force.

Over the years, the application of geosynthetics for enhancing the strength of numerous geo-structures has received significant attention [6, 7]. It includes,

*For correspondence
Published online: 07 July 2023

foundations, pavements, embankments, stability of slopes, and earth retaining structures. But very limited studies highlighted the suitability of geosynthetics reinforced foundation beds for supporting the vibration sources. Boominathan *et al* [8] revealed that the reinforcement type plays a prominent role in the dynamic response of the foundation bed through a set of vertical mode block vibration tests. Clement *et al* [9] noticed the 30% improvement in Young's modulus of the foundation bed due to the inclusion of geogrid reinforcement. Using numerical analysis, Haldar and Sivakumar Babu [10] discovered that the addition of steel reinforcement improved the natural frequency of the foundation soil system. Azzam [11] described the significant reduction in total deformation of the foundation bed with the inclusion of a confined cell, based on numerical analysis. The experimental and numerical investigation of Venkateswarlu *et al* [12] reported the advantages of geocell reinforcement over the geogrid reinforcement in enhancing the behaviour of foundation bed subjected to a vibratory load. Ujjawal *et al* [13] highlighted the advantages of honeycomb shape approach in predicting the behaviour of geocell reinforced bed under vibration load in comparison with the equivalent composite approach through a numerical investigation. Venkateswarlu and Hegde [14] examined the influence of infill material on the damping behaviour of geocell reinforced bed based on experimental and analytical investigation. Venkateswarlu *et al* [15] examined the effectiveness of a novel hybrid model (ANN-DFO) in predicting the frequency-displacement amplitude response of a footing situated on a geocell-reinforced foundation bed.

Based on thorough review of literature, existing studies majorly focussed on understanding the variation of vibration parameters and dynamic elastic constants with the change in reinforcement (geosynthetics) type, geometry of reinforcement, and thickness of the foundation bed. Although the vibration load emanated from the vibratory machines is entirely dependent on the operating frequency, none of the studies quantified the influence of frequency on isolation effectiveness and the behaviour of geocell reinforced bed. Thus, the unique and novel contribution of the present study is to explore the influence of frequency of loading on the isolation efficiency of geocell reinforced bed and vibration propagation mechanism beneath the vibration source. To demonstrate the objectives of this study, experimental and numerical analysis have been carried out. Primarily, vibration screening effectiveness of geocell reinforced bed under the influence of varying frequency has been examined through a set of field vibration tests. Using FLAC^{3D} numerical analysis, vibration propagation behaviour through the geocell reinforced bed has been analysed to bring out the underlying mechanism. Further, the effect of footing shape, geocell area, and relative density of the infill on mitigating the velocity of vibration and deformation behaviour of geocell reinforced bed has been quantified.

2. Experimental study

To study the variation of different vibration isolation indices, a series of field vibration tests were carried out over the unreinforced and geocell reinforced soil beds. A typical representation of footing situated on the geocell reinforced soil bed supporting the vibration load is shown schematically in figure 1a. A test pit of 3.6 m² and 1.2 m deep was created for preparing the unreinforced and geocell reinforced soil beds. The locally existing sand material, which is designated as silty sand (SM) based on Unified Soil Classification System was used in the preparation of both the soil beds. The grain size distribution and geotechnical properties of silty sand are shown in figure 1b. For the unreinforced bed preparation, soil was compacted layer-wise at optimum moisture content with a thickness of 0.12 m up to a total height of 1.2 m. The maximum dry unit weight and optimum moisture content of the prepared unreinforced bed were observed as 17.4 kN/m³ and 12.5%, respectively. The soil bed was reinforced using the geocell reinforcement, which is manufactured using the polymer of novel polymeric alloy. Figure 1c shows the tensile strength variation of geocell reinforcement used in the present study. Primarily, the geocell mattress was positioned at the location of 0.1B beneath the model footing. Pockets of the geocell mattress were also filled using silty sand. Figure 1d represents the partially filled geocell mattress with the silty sand material.

The detailed description of the preparation of reinforced beds was described comprehensively elsewhere by Venkateswarlu *et al* [12]. Over the prepared reinforced beds, the model footing (600 mm length, 600 mm width, and 500 mm depth) and the rotating mass type mechanical oscillator assembly was placed to apply the vibration loading. The applied vibration load simulates the vibration emanated from the rotary machines. The development of total vibration load from the rotating type of oscillator is dependent on the frequency of excitation [12].

The variation of the magnitude of dynamic force with the change in frequency of loading is shown in figure 1e. During the test, variation of peak particle velocity was assessed with the help of accelerometers and data acquisition system. Particulars of the experimental study conducted in this investigation are listed in table 1. During the field tests, the frequency of the loading was varied as 15 Hz, 25 Hz, and 45 Hz to examine the influence of frequency on the screening effectiveness of reinforced beds. The oscillator employed in this study can operate up to a frequency of 50 Hz. Accordingly, three frequencies were considered for the present investigation. It is worth mentioning that the considered frequencies are away from the natural frequency (32–40 Hz) of geocell reinforced bed [14]. Thus, resonance has no influence on the results of field tests. The square footing was employed to apply the vibration load. In the geocell reinforced condition,

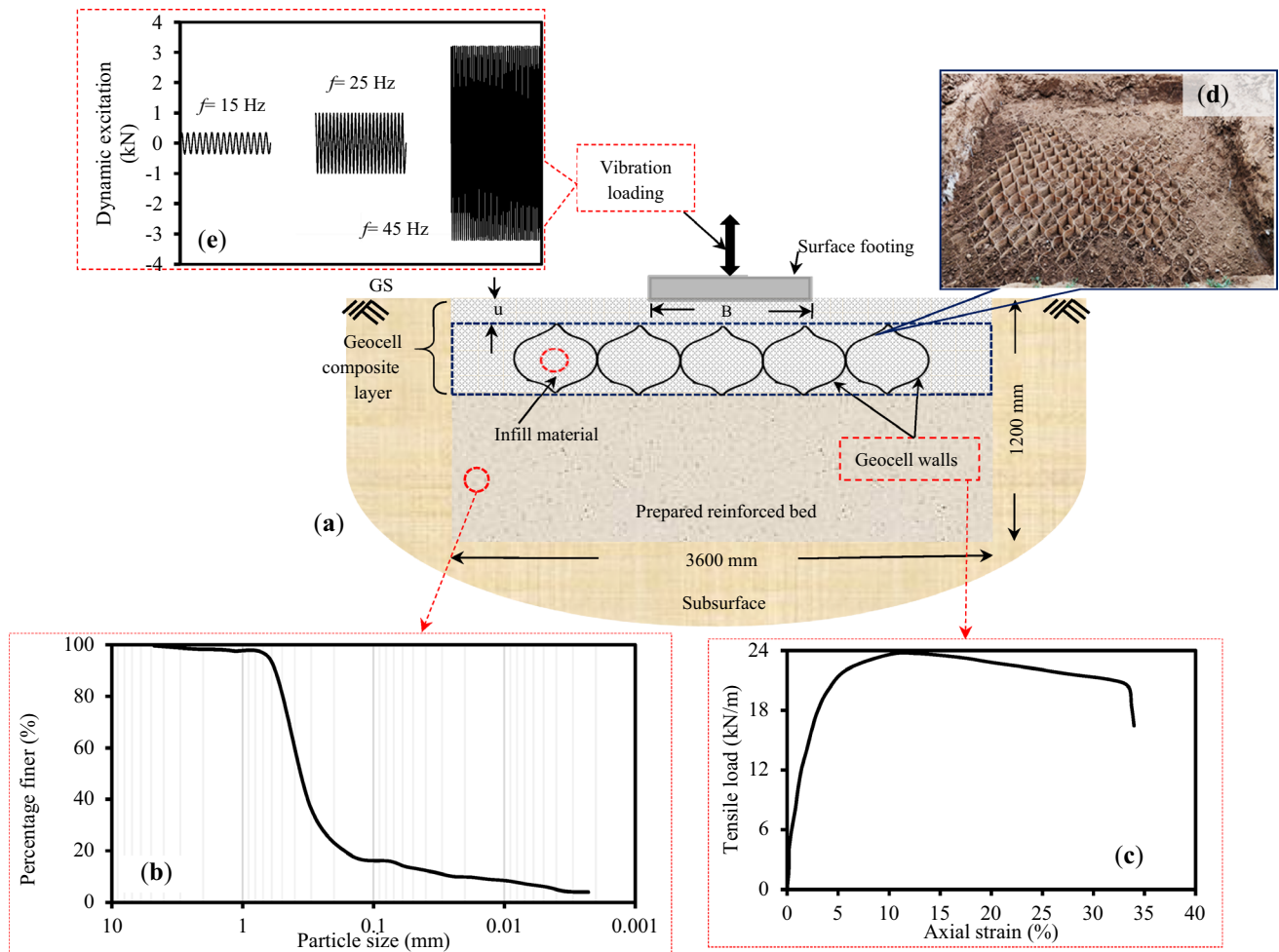


Figure 1. Details of experimental setup: (a) schematic of a reinforced bed under vibratory load; (b) particle size distribution of sand; (c) load-strain response of geocell; (d) partially filled geocell mattress; and (e) dynamic force variation with the frequency.

Table 1. Details of field tests.

Condition	Variable parameters	Constant parameters
Unreinforced	$f = 15 \text{ Hz}, 25 \text{ Hz}, \text{ and } 45 \text{ Hz}$	Square footing (length = width = 600 mm, height = 500 mm)
Geocell reinforced	$f = 15 \text{ Hz}, 25 \text{ Hz}, \text{ and } 45 \text{ Hz}$	Square footing (length = width = 600 mm, height = 500 mm); geocell area (A_g) = 9 m ²

foundation bed was reinforced with the geocell mattress having the area of 9 m² at the depth of placement of 0.1B (where B is the width of footing) from the bottom of the footing.

2.1 Experimental results

To highlight the screening effectiveness of the geocell reinforced bed, different vibration isolation descriptors were used. It includes velocity reduction ratio (VRR) and vibration mitigation efficiency (VME) as described below.

$$VRR = \frac{PPV_r}{PPV_u} \tag{1}$$

$$VME = (1 - VRR) \times 100 \tag{2}$$

where PPV_r and PPV_u represents the peak particle velocity values pertaining to the geocell reinforced and unreinforced foundation beds respectively. The maximum velocity that a soil particle can attain because of the produced vibration corresponding to three mutually orthogonal directions is referred to as peak particle velocity (PPV). Total, six accelerometers were positioned over the ground at 0.5 m

intervals from the face of the model footing in order to calculate the VRR. Typically, the foundation bed with smallest VRR and maximum VME represents highest vibration mitigation efficiency. For the unreinforced bed, the value of VRR is considered as one. Figure 2 shows the influence of frequency of loading and distance from vibration source on the VRR and VME of geocell reinforced bed.

From figure 2a, the reduction in VRR value was observed as the increase in distance from the vibration source and frequency of the excitation. Interestingly, VME was found to increase with the increase in frequency regardless of the change in distance as shown in figure 2b. This observation reveals that the role of geocell inclusion in the foundation bed is more predominant in mitigating the vibration amplitude corresponding to the higher frequencies. Generally, the vibration mitigation ability of any barrier system depends upon the wavelength (λ) of the surface wave. The wavelength (λ) of a surface wave for different frequencies i.e., 15 Hz, 25 Hz, and 45 Hz was determined as 4.86 m, 2.9 m, and 1.65 m, respectively. The wavelength decreases as the increase in excitation frequency. The low frequency vibrations spread out over a larger area owing to longer wavelengths and dissipates at a slower rate. Whereas high frequency vibration consists of

shorter wavelength which encounters the higher resistance per unit of energy as they transmitted through the foundation bed. As a result, maximum vibration energy gets dissipated in the case of higher frequency as compared to the smaller frequency. Therefore, the maximum percentage of VME was observed at the frequency of 45 Hz in comparison with the other frequencies.

On the other side, variation of attenuation coefficient (α) value for different frequencies was quantified for different test bed conditions. It is a measurement of the attenuation of vibration as a result of energy absorption as it travels through foundation beds. The higher the value of α suggests the better attenuation capacity of a system. To determine the α , the acceleration response of two accelerometers arranged at the locations of 1.5 m and 3 m from the vibration source was used. These accelerometers were positioned in the same line along the longitudinal direction. The attenuation coefficient was calculated using the following expression as provided by IS 5249 [16].

$$\alpha = \frac{1}{(d_2 - d_1)} \ln \left[\frac{A_2}{A_1} \sqrt{\frac{d_2}{d_1}} \right] \quad (3)$$

where A_1 and

A_2 are the velocity of vibration at the distances of d_1 and d_2 respectively. Variation of attenuation coefficient for unreinforced and geocell reinforced beds is shown in figure 3. In both cases, increase in attenuation coefficient was observed with the increase in frequency. However, maximum attenuation coefficient was noticed in the presence of geocell reinforced bed as compared to the unreinforced bed. This observation highlights that the provision of geocell has a significant influence on improving the vibration attenuation ability of the foundation bed. The emanated surface waves from the vibration source get diffracted into a wider region by the geocell mattress. Consequently, the energy of induced vibration gets further attenuated.

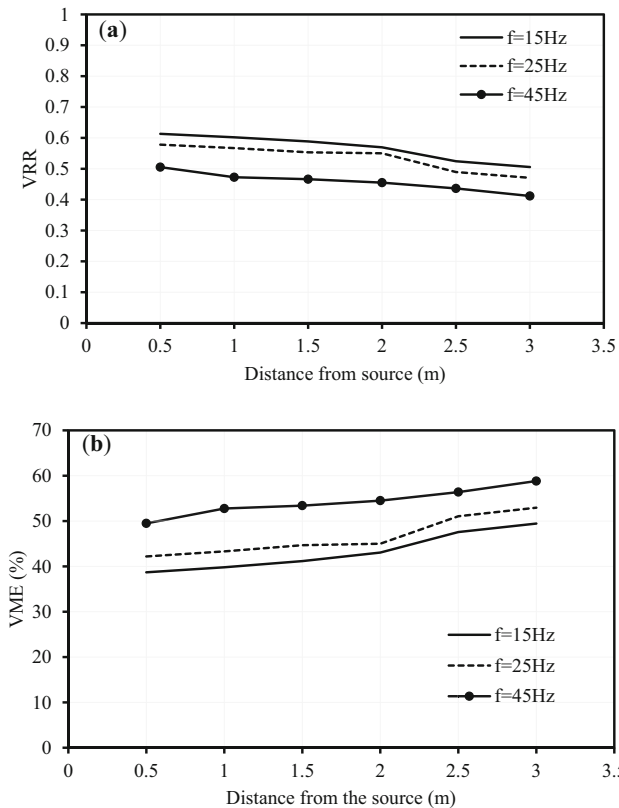


Figure 2. Influence of frequency and distance from vibration source on the variation of vibration isolation parameters: (a) VRR; and (b) VME.

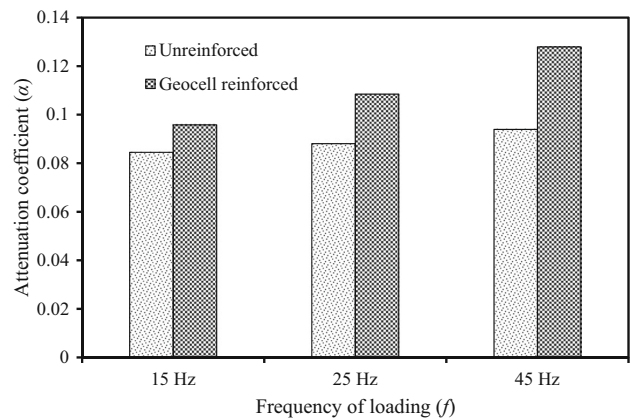


Figure 3. Influence of frequency on the attenuation coefficient of different soil beds.

3. Numerical modeling

Continuum approach-based finite-difference package FLAC^{3D} was employed for the numerical investigation. To evaluate a particular problem, FLAC3D discretizes it into minor steps (Itasca, 2008). It has been widely used for analyzing complex geotechnical problems due to the availability of diverse constitutive models and structural elements (SEs). The built-in interface component aids in simulating the behaviour of interaction between two diverse materials. Additionally, it has a robustly integrated programming language named FLACish that can be used to create new functions and variables. Numerous studies have described the possible benefits of FLAC in quantifying the behaviour of foundation beds under dynamic and vibration loading [10, 12, 17, 18].

In the numerical analysis, precise quantification of the modeling parameters of different test materials is very essential for obtaining the realistic output from the developed numerical model. Gazetas [19] stated that the consideration of native subsurface profile is crucial in quantifying the response of foundation beds under vibration loading. Therefore, parameters corresponding to subsurface and reinforced beds were determined and considered into account during the modeling. Figure 4 shows the developed numerical model for geocell reinforced case. The input modeling parameters of the foundation system are listed in table 2. While analyzing the geocell reinforced bed, geocell pockets were infilled with the sand at different relative densities i.e., 60%, 75% and 85% (denoted by sand₁, sand₂ and sand₃, respectively). The different modeling parameters

Table 2. Modeling parameters of reinforced bed.

Material	Modeling parameter	Quantity
Model footing	Modulus of elasticity of concrete (MPa)	2×10^4
	Unit weight of concrete (kN/m ³)	24
	Poisson's ratio of concrete	0.15
Geocell	Young's modulus (MPa)	275
	Poisson's ratio	0.45
	Thickness (mm)	1.5
Sand ₁	Relative density (%)	60
	Cohesion (kPa)	0
	Internal friction (°)	30
	Unit weight (kN/m ³)	16.3
	Young's modulus (MPa)	22
	Interface cohesion, c_i (kPa)	0
	Interface friction angle, ϕ_i (°)	27
Sand ₂	Relative density (%)	75
	Cohesion (kPa)	0
	Internal friction (°)	36
	Unit weight (kN/m ³)	17.8
	Young's modulus (MPa)	38
	Interface cohesion, c_i (kPa)	0
	Interface friction angle, ϕ_i (°)	31
Sand ₃	Relative density (%)	85
	Cohesion (kPa)	0
	Internal friction (°)	39
	Unit weight (kN/m ³)	18.3
	Young's modulus (MPa)	43
	Interface cohesion, c_i (kPa)	0
	Interface friction angle, ϕ_i (°)	34

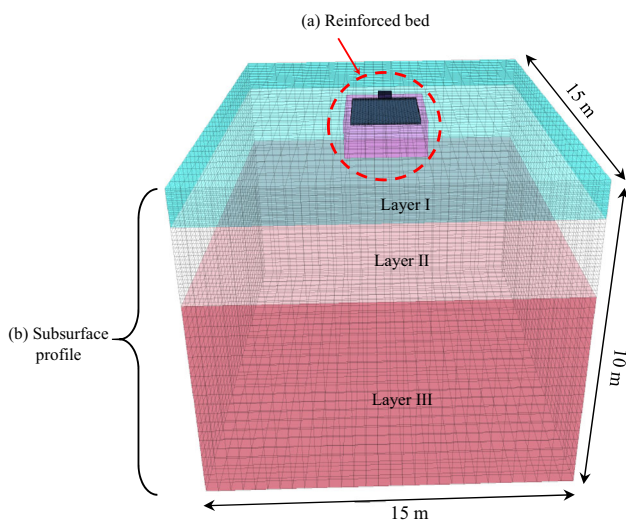


Figure 4. Finite difference model of geocell reinforced bed with subsurface profile. Note: B represents width of footing; L indicates the length of a geocell reinforced bed; H is depth of a geocell reinforced bed; h is height of geocell reinforcement; b indicates width of geocell reinforcement; u indicates placement depth of geocell beneath the footing.

of sand infill corresponding to each relative density are also listed in table 2. All the listed properties were determined using the series of laboratory experiments. Whereas table 3 highlights the modeling parameters of the subsurface profile. The dimensions of the reinforced bed were considered as like the field test conditions. To develop the unreinforced and geocell reinforced beds, the available brick element in FLAC3D was employed. As per the sensitivity analysis, the optimum dimensions of the numerical model were chosen as 15 m × 15 m × 10 m. The coarse mesh following the 18000 numbers of zones was used.

The elastic and perfectly plastic Mohr-Coulomb constitutive behaviour was selected to simulate the behaviour of subsurface soil layers and the foundation soil. Model footing was considered to obey the behaviour of elastic material. The propagation of vibration in the lateral direction was restricted at the vertical faces of the model. Vibration propagation was restricted in all directions at the bottom face of the developed model. Additionally, all the vertical faces and bottom face were assigned with quiet (viscous) boundaries to implement the far-field circumstances. These boundary conditions have the advantage of preventing wave reflections returning into the soil medium from a model boundary. For the foundation bed and all

Table 3. Modeling parameters of subsurface [13].

Stratum	Modeling parameter	Quantity
Layer-I: Silty clay (0 m–1.1 m)	Cohesion (kPa)	48
	Internal friction (°)	3
	Dynamic modulus (MPa)	38.2
	Unit weight (kN/m ³)	16.3
Layer-II: Loose sand (1.1 m–2.35 m)	Cohesion (kPa)	1
	Internal friction (°)	30
	Dynamic modulus (MPa)	151
	Unit weight (kN/m ³)	17.8
Layer-III: Dense sand (2.35 m–10 m)	Cohesion (kPa)	1
	Internal friction (°)	36
	Dynamic modulus (MPa)	256
	Unit weight (kN/m ³)	256

subsurface layers, a material damping of 5% was considered [20]. It signifies the dissipation behaviour of induced vibration during the transmission through the soil layers. Various researchers have adopted a similar methodology for analyzing the foundations under dynamic loading conditions [18, 21].

While modeling the reinforced bed, actual honeycomb shape of the geocell reinforcement was considered. For this purpose, the digitization approach suggested by Hegde and Sitharam [22] was followed. Regardless of the stress state, walls of the geocell mattress behave as a tension membrane. Thus, to replicate the geocell, the built-in geogrid structural component was utilized. It is a triangular element with constant strain that can withstand tensile pressures. To model the actual response of geocell composite layer, two distinct constitutive behaviours were assigned to the geocell reinforcement and the infill material. For modelling the

infill materials and the soil-geocell wall interface, the Mohr-Coulomb constitutive behaviour was chosen. Geocell was modeled to obey linear elastic behaviour [22]. It is worth noting that the sand was used as the infill material to fill the geocell pockets in the numerical modeling.

Table 4 summarizes the analysis carried out in the numerical investigation. All the invariable parameters for the condition of geocell reinforced bed subjected to a vibration load is shown schematically in figure 5. The primary aim of a first two series of analyses is to understand the variation of VRR with the change in footing shape. Moreover, the influence of frequency on the shear strain behaviour of unreinforced and geocell reinforced foundation beds was also quantified. Based on series III, the effect of geocell area on the VRR was quantified. Whereas the effect of relative density of infill, frequency of loading on the variation of VRR and shear strain response was studied from the analysis of series IV. Also, the vibration propagation pattern through the geocell reinforced bed was described. Based on the vibration transmission pattern, possible justification for the mitigation of vibration energy was demonstrated. In the analysis of geocell reinforced soil beds, the width and depth of placement of geocell were maintained constant as $5B$ and $0.1B$ respectively. These parameters were reported as optimum to achieve the highest isolation effectiveness in the past [23]. Both the unreinforced and geocell reinforced beds were examined under the vertical mode rotating mass type dynamic excitation. During the analysis, the dynamic force was run for 10 s. The developed model was suitably validated before performing the numerical analysis. To do so, experimentally observed VRR response equivalent to the frequency of 45 Hz was compared as shown in figure 6. It is worth mentioning that the geometry of a reinforced bed, and the properties of soil material similar to the one discussed in the experimental study have been used in the validation.

Table 4. Particulars of numerical analysis.

Series	Type of soil bed	Variable particulars		Invariable particulars
		Parameter	Values/details	
I	Unreinforced	Footing shape Frequency;	Square and rectangle 15 Hz; 25 Hz and 45 Hz	$L = 6B; H = 2B$
II	Geocell	Footing shape Frequency;	Square and rectangle 15 Hz; 25 Hz and 45 Hz	Footing height: 500 mm; Geocell area = 9 m ² ; Relative density of sand infill = 75%
III	Geocell	Area of geocell mattress	2.4 m × 2.4 m; 3 m × 3 m and 3.6 m × 3.6 m	Square footing $b = 5B; h = 0.12B; u = 0.1B$; square footing; Relative density of sand infill = 75%
IV	Geocell	Frequency; Relative density of infill	15 Hz; 25 Hz and 45 Hz 60%, 75% and 85%	$b = 5B; h = 0.12B; u = 0.1B$; square footing; Geocell area = 9 m ²
		Frequency	15 Hz; 25 Hz and 45 Hz	

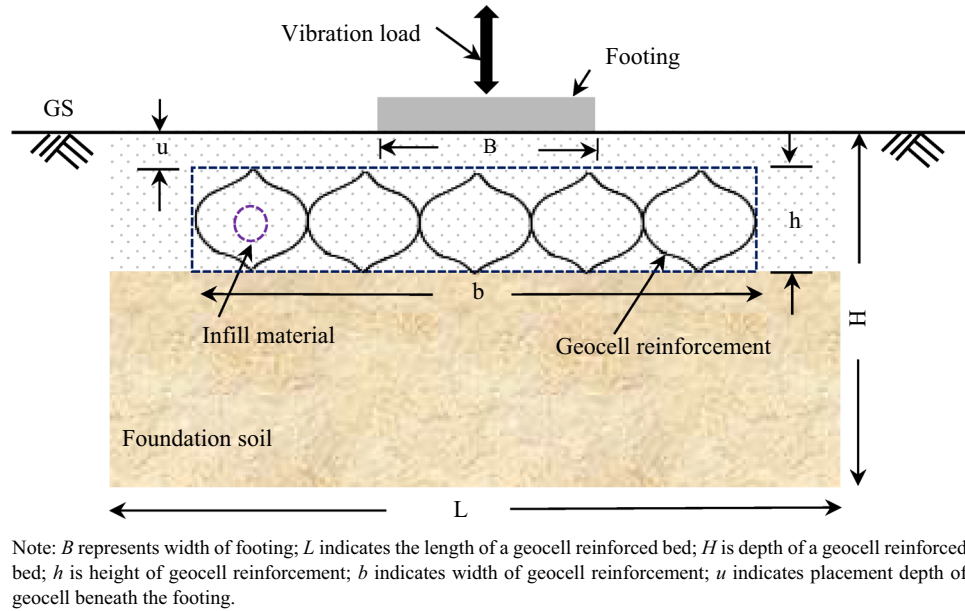


Figure 5. Schematic representation of numerous invariable parameters for the case of geocell reinforced bed under vibration load.

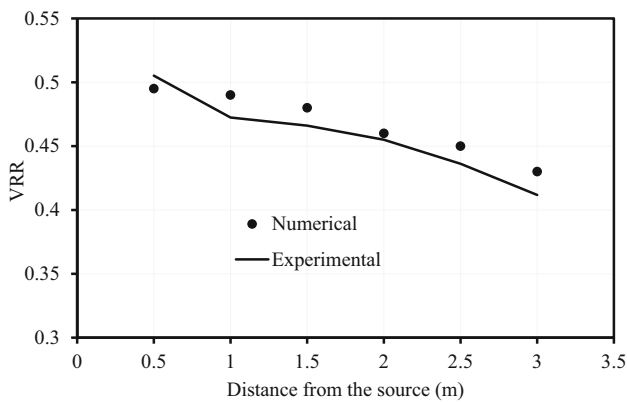


Figure 6. Comparison of VRR response obtained from numerical and experimental studies.

From figure 6, a reasonable agreement between the numerical and experimental results was observed. Regardless of the distance, less than a 5% deviation was noted between the experimental and numerical VRR values. It highlights that the developed models can predict the realistic performance of reinforced soil beds under vibration loading. Therefore, the validated models were further used for performing the numerical investigation as per the methodology listed in table 4.

3.1 Effect of footing shape on VRR and strain response

In general, the shape of footing can exhibit a significant influence on wave propagation behaviour. To understand

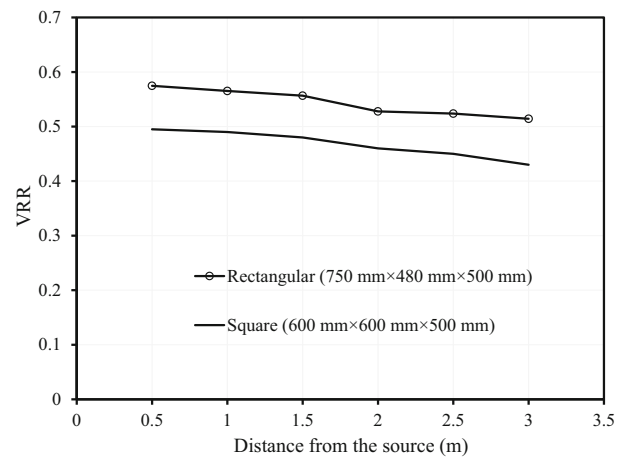


Figure 7. Influence of footing shape on VRR

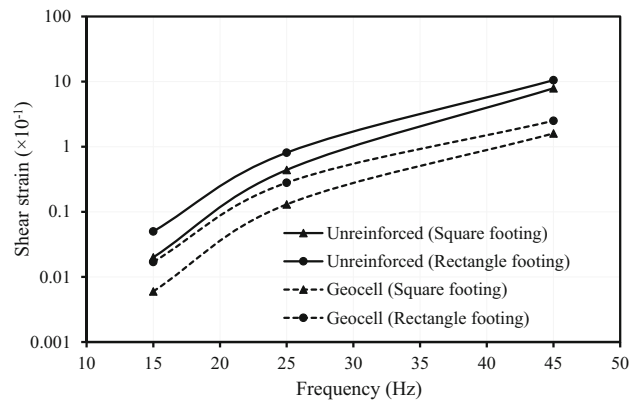


Figure 8. Influence of footing shape on the shear strain of foundation beds.

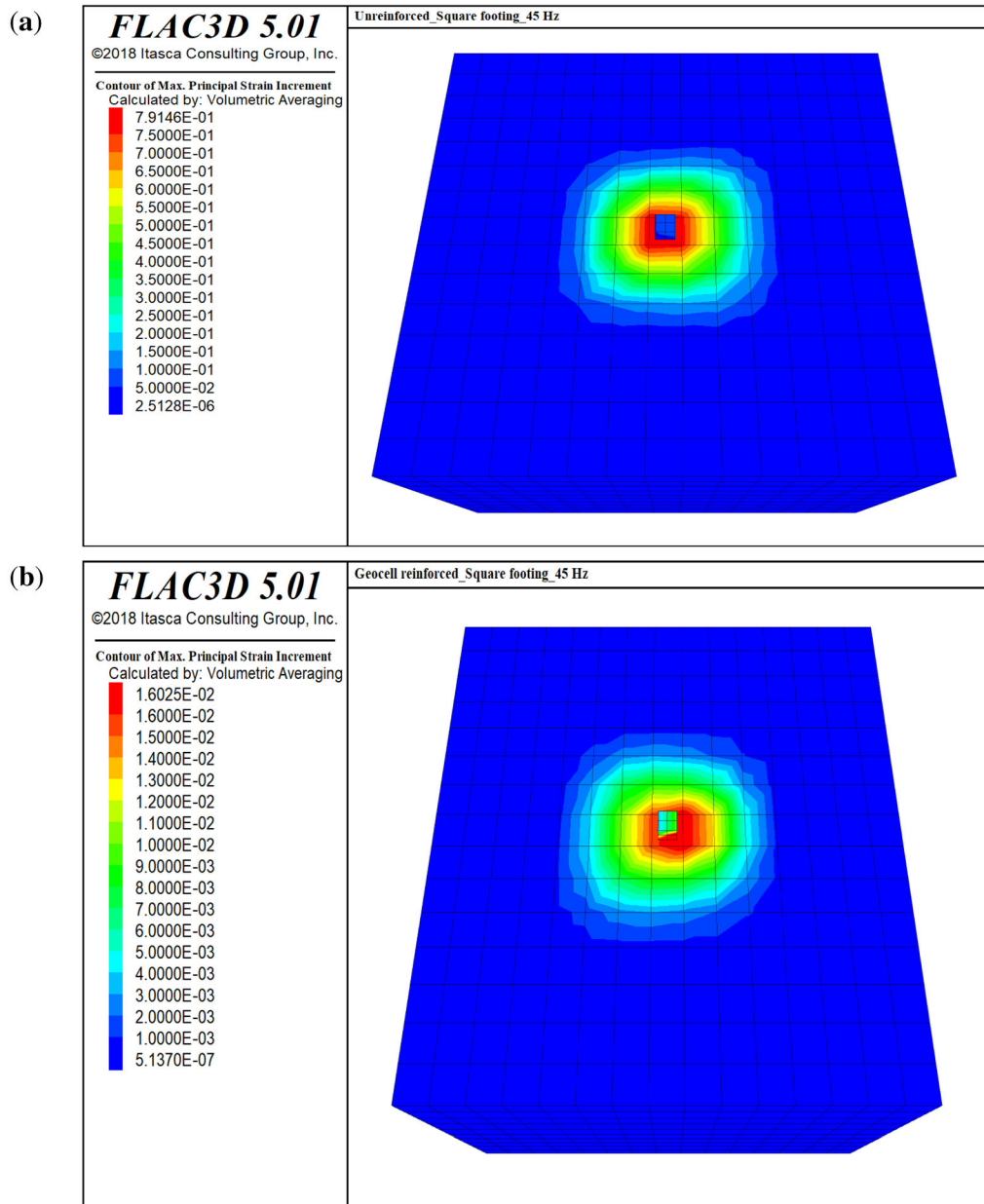


Figure 9. Strain contours of foundation beds supporting square footing at frequency of 45 Hz: (a) unreinforced bed; (b) geocell reinforced bed.

this effect, variation of VRR for different footing shapes is shown in figure 7. Two different types of footing shapes namely, square, and rectangular with 500 mm in height were used in the analysis. The volume of square footing was considered constant to determine the base area of the rectangular footing. From the figure, a lower VRR value was noticed in the case of square footing in comparison with the rectangular footing regardless of the increase in distance from the vibration source. It was mainly attributed due to the changes in the interaction behaviour between the footing area and reinforced bed with the

variation in footing shape. In the case of rectangular footing, disturbance created over the foundation bed might be higher due to the unequal dimensions of length and width. As a result, shear strength of soil mass close to the footing gets disturbed and eventually effect the damping behaviour. It leads to the decrease in attenuation ability and resulted in higher VRR values. Whereas disturbance of the foundation bed is less in the presence of square footing by the virtue of equal dimensions. It leads to the lower VRR values as compared to the rectangular footing. It provides an insight that the utilization of square footing

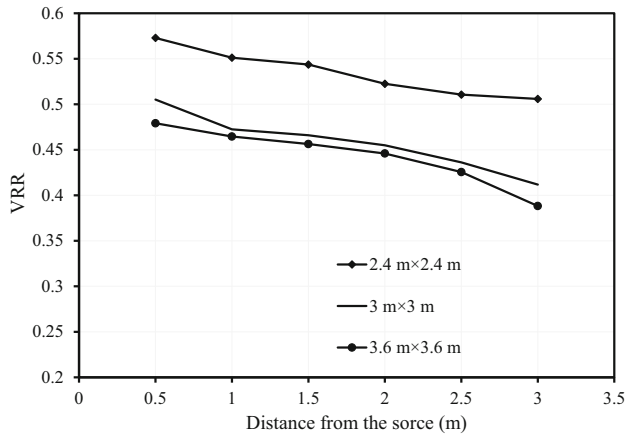


Figure 10. Variation of VRR with the change in the area of geocell mattress.

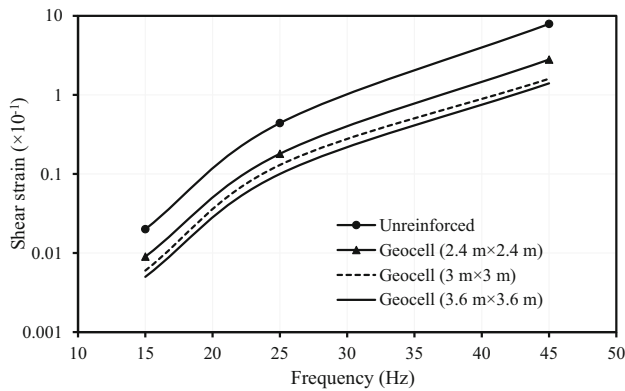


Figure 11. Influence of geocell area on the shear strain of reinforced beds.

is more effective for controlling the vibration effect than rectangular footing.

Further, foundation beds supporting the vibration sources are subjected to a wide range of dynamic shear strain levels. The mobilized dynamic shear strain can distinctly affect the different dynamic properties like dynamic shear modulus and damping ratio. Thus, quantification of the magnitude of shear strain experienced by the foundation bed under vibration loading is very important. The variation in shear strain of different reinforced beds with the variation in footing shape is shown in figure 8. Regardless of the footing shape, the shear strain developed over the geocell reinforced bed was found less as compared to the unreinforced bed. It was primarily caused by the significant increase in the elastic response of the foundation bed because of the provision of geocell [12, 17, 24]. Also, the magnitude of shear strain was increased with the increase in frequency of excitation. Moreover, both the unreinforced and geocell reinforced beds were experienced lower shear strain values under the square footing. Thus, the utilization of square shaped footing over the rectangle shape is more

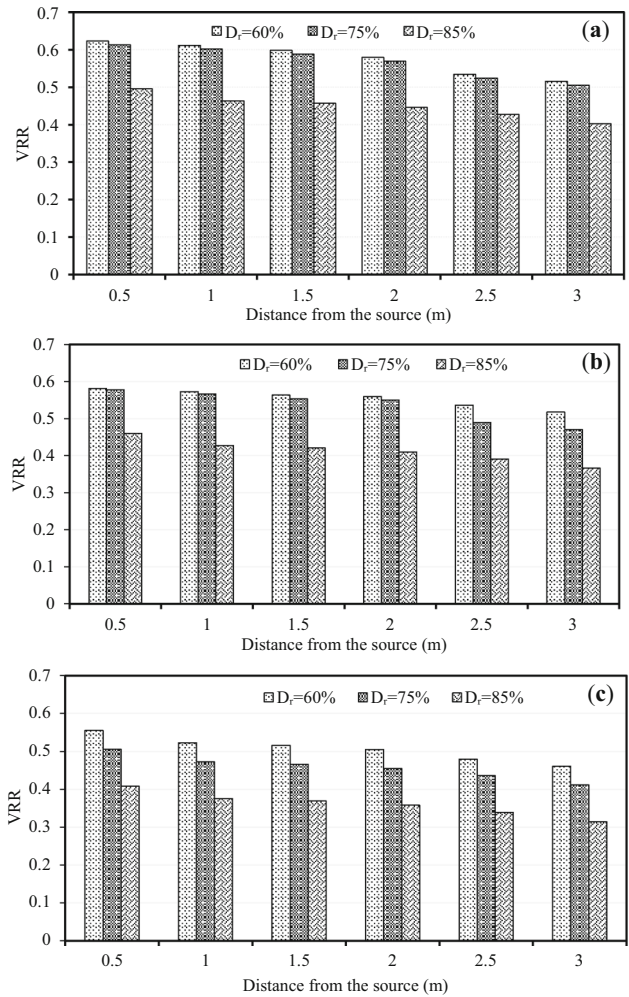


Figure 12. Influence of relative density of infill on the variation of VRR at different frequencies: (a) 15 Hz; (b) 25 Hz; and (c) 45 Hz.

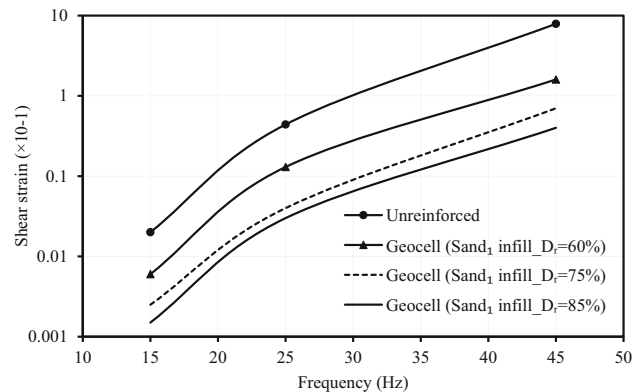


Figure 13. Strain variation over the reinforced bed with the change in relative density of infill.

effective for the vibration propagation. The observed strain contours for unreinforced and geocell reinforced beds supporting the square footing at the frequency of 45 Hz are shown in figure 9 for demonstration purpose.

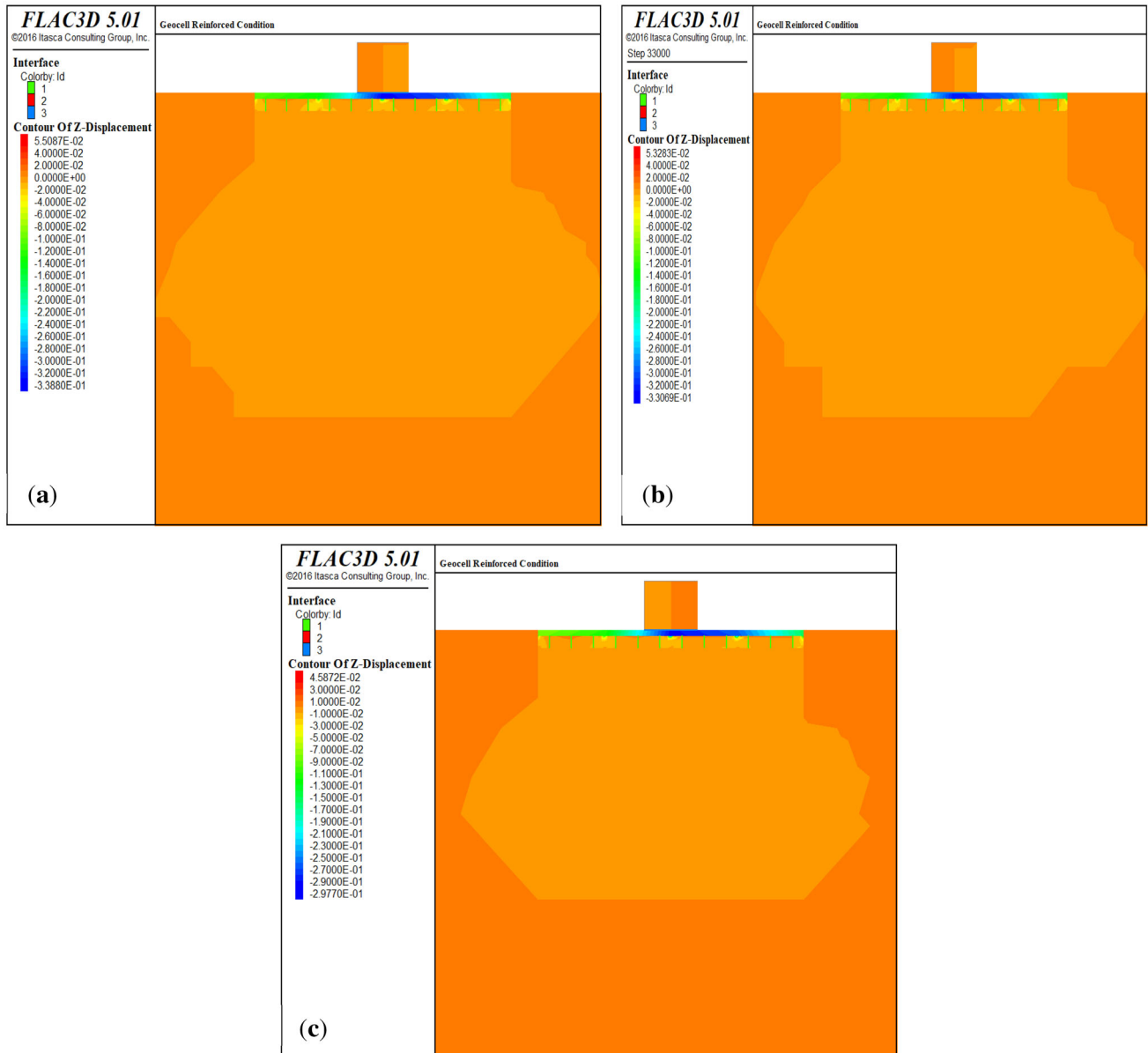


Figure 14. Displacement contours of geocell reinforced bed at different frequencies: (a) 15 Hz; (b) 25 Hz; and (c) 45 Hz.

3.2 Effect of geocell area on VRR and strain response

Figure 10 shows the variation of VRR with the change in the area of geocell mattress. The VRR was found to decrease with the increase in geocell area and the distance from the vibration source. The decreasing trend of VRR signifies the role of the area of geocell in decaying the energy of produced vibration. As the increase in geocell area, the overall confined area increases in the foundation bed. It results in the increase in attenuation ability of the foundation bed. Thus,

the lower values of VRR were noticed when the foundation bed reinforced with larger geocell mattress.

The influence of geocell area on the developed shear strain of geocell reinforced bed is shown in figure 11. The magnitude of shear strain corresponding to the geocell reinforced bed was further reduced with the increase in the area of geocell mattress. Regardless of operating frequency, more than 54%, 70%, and 75% decrease in the shear strain of the foundation bed was noticed when it is reinforced with the geocell area of 5.76 m², 9 m² and 12.96 m² respectively.

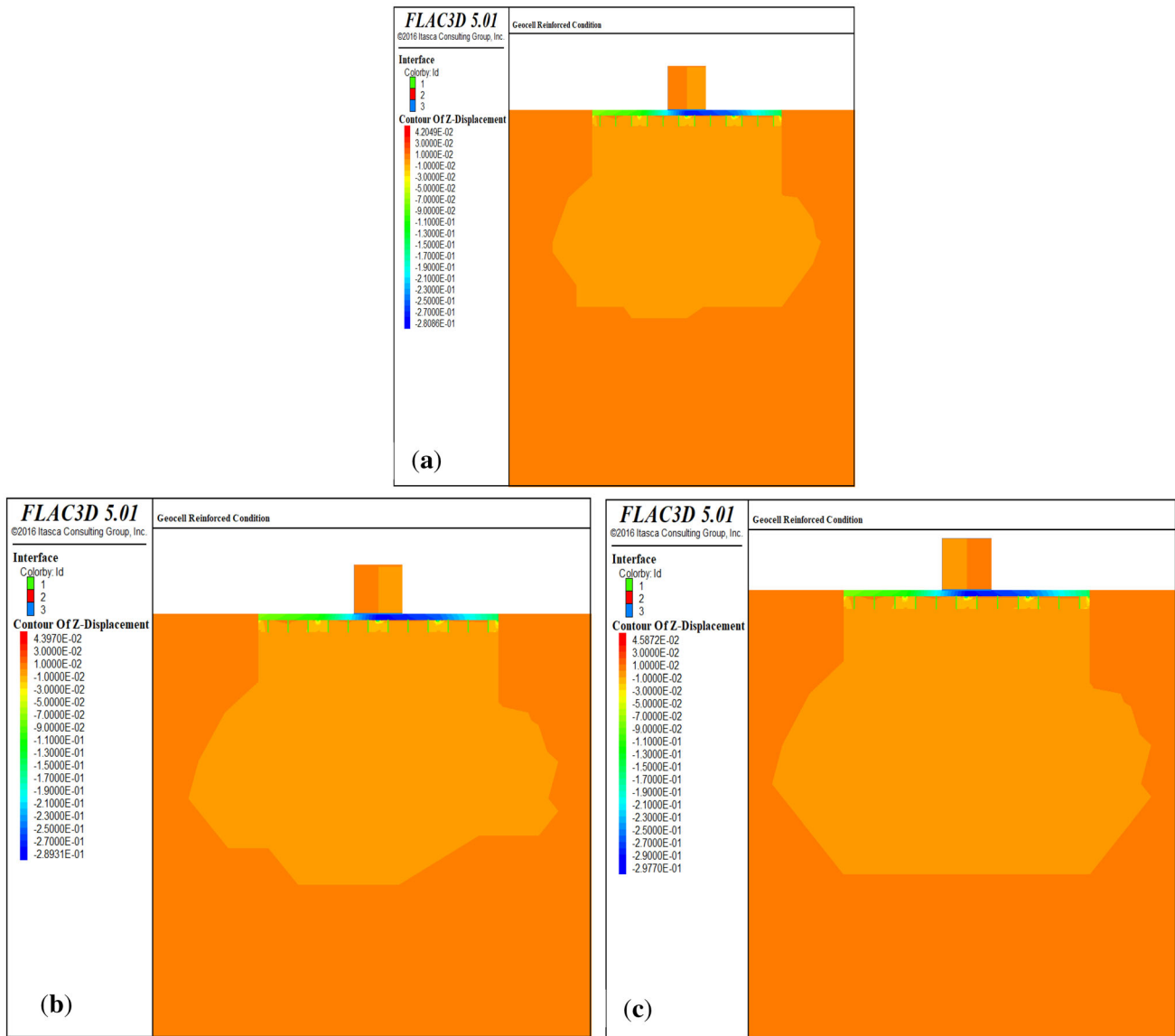


Figure 15. Displacement contours of geocell reinforced bed at different relative densities of sand infill: (a) $Dr = 60\%$; (b) $Dr = 75\%$; and (c) $Dr = 85\%$.

3.3 Effect of relative density of infill on VRR and strain response

Figure 12 shows the influence of frequency of loading on the variation of VRR with the change in relative density of infill material. For this purpose, the relative density of sand was considered as 60%, 75%, and 85%. Different modelling parameters corresponding to each relative density of sand is provided in table 2. With the increase in relative density of the infill, the VRR value was found to decrease regardless of the frequency. Whereas, a lower value of VRR was noted at the frequency of 45 Hz in comparison with the 30 Hz and 15 Hz frequency irrespective of the relative density of infill.

Variation of shear strain over the reinforced bed at different frequencies and relative densities of infill is shown in figure 13. The shear strain over the reinforced bed was decreased further with the increase in the relative density of infill material. Irrespective of frequency, a percentage reduction in shear strain was observed by more than 75%, 88%, and 93% respectively at the relative density of 60%, 75%, and 85% as compared to the unreinforced bed. It was attributed due to the distinct increase in elastic response with the increase in relative density. Tafreshi *et al* [17] has also noticed the increase in the elastic response of a geocell reinforced bed with the increase in the relative density of the infill.

3.4 Displacement contours

Experimental and numerical results revealed that the generated vibration energy distinctly decays in the case of geocell reinforced bed as compared to unreinforced bed. Understanding the propagation behaviour of induced vibration provides an insight about the decay of produced vibration in the case of geocell reinforced bed. For this purpose, variation of displacement contours beneath the geocell mattress were observed at different frequencies. Displacement contours are resulted due to transmission of produced vibration through the reinforced bed with the time. Thus, displacement contours in a way useful to capture the propagation behaviour of vibration. Displacement contours corresponding to different frequencies of loading is shown in figure 14. The reported contours are related to the scenario of geocell pockets infilled with the sand at the relative density of 85%.

The induced vibration was found to propagate into a wider area beneath the geocell mattress. Interestingly, the induced vibration corresponding to the frequency of 15 Hz was transmitted to greater depth beneath the geocell as compared to the frequencies of 25 Hz and 45 Hz. The depth of transmission decreases with the increase in frequency. It reveals that the role of geocell is significant for the efficient isolation of vibration energy at a higher frequency. Generally, vibration corresponding to a lower frequency consists of a higher wavelength. It results in the decay of vibration at a slow rate. As a result, a greater depth of transmission was observed at the frequency of 15 Hz (as shown in figure 14a). Ultimately, propagation of vibration into a wider area helps to dissipate the maximum amount of vibration energy. Thus, the lower values of VRR were noticed. Figure 15 shows the displacement contours of geocell reinforced bed with the variation in relative density of infill at the frequency of 45 Hz.

The propagated area of induced vibration beneath the geocell was increased with the increase in relative density of infill material. It highlights that filling the geocell pockets at a higher relative density significantly improves the mitigation ability of vibration energy. Based on this mechanism, lower values of VRR were noticed in the geocell reinforced case having the infill of higher relative density (refer to figure 12).

4. Conclusions

The present study emphasized the influence of frequency of loading on the screening efficacy, vibration propagation and deformation behaviour of the geocell reinforced bed using the experimental and FLAC3D based numerical investigation. Experimental results demonstrated that the isolation efficacy of the geocell is more prominent in higher frequencies. Irrespective of the distance from the vibration source, vibration mitigation efficiency (VME)

corresponding to the frequency of 45 Hz was observed by more than 50%. Similarly, the velocity attenuation coefficient of the foundation bed was increased distinctly with the inclusion of geocell reinforcement. In comparison with the unreinforced bed, percentage increase in attenuation coefficient of the geocell reinforced bed was increased from 14 to 42% with the increase in frequency from 15 to 45 Hz. Based on the numerical results, the effect of vibration was found minimum in case of square footing as compared to rectangular footing. The value of VRR pertaining to the geocell reinforced soil bed was found to reduce with the increase in the area of geocell mattress and relative density of the infill material. The strain-induced over the foundation bed was found to increase with the increase in frequency regardless of the reinforced bed. However, foundation bed strain was distinctly controlled due to the inclusion of geocell. Regardless of the frequency and relative density of the infill, more than 75% decrease in strain over the foundation bed was observed due to the inclusion of geocell reinforcement. Displacement contours highlighted that geocell reinforcement enhances the vibration mitigation efficacy by propagating the induced vibration into a wider area.

References

- [1] Ding G, Sun F and Fu H 2019 Vibration propagation of diverse footings on saturated sand. *Int. J. Civ. Eng.* 17(2): 265–279
- [2] Matešić L and Vucetic M 2003 Strain-rate effect on soil secant shear modulus at small cyclic strains. *J. Geotech. Geoenviron. Eng.* 129(6): 536–549
- [3] Baidya D K and Rathi A 2004 Dynamic response of footings resting on a sand layer of finite thickness. *J. Geotech. Geoenviron. Eng.* 130(6): 651–655
- [4] Kumar J and Reddy C O 2006 Dynamic response of footing and machine with spring mounting base. *Geotech. Geol. Eng.* 24(1): 15–27
- [5] Kirar B, Krishana A M and Rangwala H M 2015 Dynamic properties of soils for the design of machine foundations. *Proceedings of Indian Geotechnical Conference*, Chennai, India, December, 1–4
- [6] Ferreira F B, Vieira C S, Lopes M L and Carlos D M 2016 Experimental investigation on the pullout behaviour of geosynthetics embedded in a granite residual soil. *Eur. J. Environ. Civ. Eng.* 20(9): 1147–1180
- [7] Hegde A 2017 Geocell reinforced foundation beds-past findings, present trends and future prospects: a state-of-the-art review. *Constr. Build. Mater.* 154: 658–674
- [8] Boominathan S, Senathipathi K and Jayaprakasam V 1991 Field studies on dynamic properties of reinforced earth. *Soil Dyn. Earthq. Eng.* 10(8): 402–406
- [9] Clement S 2015 Experimental Studies on Dynamic Response of a Block Foundation on Sand Reinforced with Geogrid. *Geosynthetics 2015*, February 15–18, Portland, Oregon, 479–488

- [10] Haldar S and Sivakumar Babu G L 2009 Improvement of machine foundations using reinforcement. *Proc. Inst. Civ. Eng.-Ground Improv.* 162(4): 199–204
- [11] Azzam W R 2015 Utilization of the confined cell for improving the machine foundation behavior-numerical study. *J. GeoEng.* 10(1): 17–23
- [12] Venkateswarlu H, Ujjawal K N and Hegde A 2018 Laboratory and numerical investigation of machine foundations reinforced with geogrids and geocells. *Geotext. Geomembr.* 46(6): 882–896
- [13] Ujjawal K N, Venkateswarlu H and Hegde A 2019 Vibration isolation using 3D cellular confinement system: A numerical investigation. *Soil Dyn. Earthq. Eng.* 119: 220–234
- [14] Venkateswarlu H and Hegde A 2020 Effect of infill materials on vibration isolation efficacy of geocell-reinforced soil beds. *Can Geotech. J.* 57(9): 1304–1319
- [15] Hasthi V, Raja M N A, Hegde A and Shukla S K 2022 Experimental and Intelligent Modelling for Predicting the Amplitude of Footing Resting on Geocell-Reinforced Soil Bed under Vibratory Load. *Transportation Geotechnics*, 100783
- [16] Indian Standard Code 5249 1992 *Determination of dynamic properties of soil-method of test.* Prabhat Offset Press, Delhi, India
- [17] Tafreshi S M, Zarei S E and Soltanpour Y 2008 Cyclic loading on foundation to evaluate the coefficient of elastic uniform compression of sand. In: *The 14th world conference on earthquake engineering*, Beijing, China
- [18] Moghaddas Tafreshi S N, Tavakoli Mehrjardi G and Ahmadi M 2011 Experimental and numerical investigation on circular footing subjected to incremental cyclic loads. *Int. J. Civ. Eng.* 9(4): 265–274
- [19] Gazetas G 1991 Formulas and charts for impedances of surface and embedded foundations. *J. Geotech. Eng.* 117(9): 1363–1381
- [20] Richart F E, Woods R D, Hall J R and Jr 1970 *Vibrations of soils and foundation.* Prentice-Hall, Inc., Englewood Cliffs, N.J
- [21] Venkateswarlu H and Hegde A 2022 Behavior of Geocell Reinforced Bed Subjected to Vibration Loading: 3D Numerical Studies. *Geosynth. Int.*, 1–54
- [22] Hegde A and Sitharam T G 2015 3-Dimensional numerical modelling of geocell reinforced sand beds. *Geotext. Geomembr.* 43(2): 171–181
- [23] Venkateswarlu H and Hegde A 2020 Effect of influencing parameters on the vibration isolation efficacy of geocell reinforced soil beds. *Int. J. Geosynth. Ground Eng.* 6: 1–17
- [24] Venkateswarlu H and Hegde A 2020 Isolation prospects of geosynthetics reinforced soil beds subjected to vibration loading: experimental and analytical studies. *Geotech. Geol. Eng.* 38(6): 6447–6465